LA-UR-01-2085
Approved for public release;
distribution is unlimited.

Title: **Advanced Silicide-Based Materials for High Temperature Glass Processing Sensors**

Author(s): Richard G. Castro, Maria I. Peters, Daniel E. Mendoza, Rajendra U. Vaidya , John J. Petrovic

Submitted to:

http://lib-www.lanl.gov/la-pubs/00818577.pdf

Advanced Silicide-Based Materials for High Temperature Glass Processing Sensors

Richard G. Castro, Maria I. Peters, Daniel E. Mendoza, Rajendra U. Vaidya , John J. Petrovic,

Materials Science and Technology Division
Los Alamos National Laboratory

1.0 ABSTRACT

Materials research is needed to improve the performance of high temperature materials that must withstand the hostile environment of the glassmaking process and to improve the operating efficiency. Advances in materials used for sensors and controls is perhaps one of the most important requirements for improving the efficiency of the glass production process. The use of molybdenum disilicide ($MoSi_2$) based materials, which are corrosion resistant in glass, are being investigated for improving the performance of advance temperature sensors. Using advanced plasma spray forming techniques, laminate and functionally graded composite tubes of $MoSi_2$ and Al_2O_3 are being developed to protect advanced temperature sensors from the hostile environment of the glassmaking process.

2.0 INTRODUCTION

In 1994, the glass industry consumed over 200 trillion Btu's of process energy **[1].** Approximately 83 percent of this energy was in the form of natural gas, 13 percent in the form of electricity, and the remaining 4 percent in the form of residual and distillated fuel oil. Whereas melting one ton of glass should theoretically require only about 2.2 million Btu's, in practice it requires a minimum of twice that much because of the variety of losses and inefficiencies in the glass melting process **[1].** Temperature sensors play an important role in controlling the melt processing of glass but as a consequence of the degradation and inefficiency of the temperature sensor, significant energy consumption can result. Increasing energy consumption results in an increase in the particulate emissions of CO_2, NO_x and SO_x. Glass melting operations have resulted in the production of approximately 30,000 metric tons of CO_2, NO_x and SO_x **[1**]. One of the major objectives of the glass industry of the future is to improve the temperature sensors used in the melting of glass in order to help reduce energy consumption and improve the operating efficiency.

Three major problem areas associated with temperature measurement technology are; 1) uncertain, "drifting" temperature data, 2) short sensor life due to the failure of the internal components of the temperature sensor and 3) short sensor life due to the failure of the protective sheath material. An example of the drift that is associated with metal-sheathed noble-metal thermocouples measured at 1305 ^{o}C over a period of minutes is given in **Figure 1**. The drift in temperature is directly associated with the type of sheathed material used to protect the thermocouple.

When selecting a protective sheath material for a glass temperature sensor a number of factors need to be considered including; the chemical stability of the sheath material in the glass processing environment (above the glass, below the glass and at the glass line), the potential contamination of the glass from the sheath material, decalibration of the temperature sensor due to impurity migration from the sheath material and the mechanical and thermal shock performance of the sheath material in the aggressive glass melting process. The use of platinum coatings on alumina (Al_2O_3) sheaths for thermocouples is a widely employed practice in the glass industry. The cost associated with providing platinum coatings on the Al_2O_3 sheath material can be prohibitively high when taking into consideration the infrastructure needed at the glass plants to maintain and secure an inventory of available platinum. There are also issues associated with improving the performance of the platinum coated Al_2O_3. The failure rate due to thermal shock of the thermocouples can be as high as 50%. The U.S. glass industry has been in search of alternative materials that can replace platinum and still provide the durability and performance needed to survive in an extremely corrosive glass environment.

Investigations by Y.S. Park et al **[3**] have shown that molybdenum disilicide ($MoSi_2$) has similar performance properties in molten glass as some refractory materials that are currently being used in glass processing applications. Above the glass line $MoSi_2$ forms a protective SiO_2 layer preventing oxidation of the material. Below the glass line molybdenum rich phases (Mo_5Si_3) can form which enhances the performance of the material when in contact with the molten glass. A thermodynamic analysis of equilibrium amounts of various materials in silica between 1000 ^oC and 2800 ^oC is shown in **Figure 2**. From this analysis Pt, Mo_5Si_3, Cr_2O_3, Mo and $MoSi_2$ are relatively stable when in contact with molten SiO_2.

Plasma spraying has been demonstrated by a number of researchers **[4,5,6,7]** to be a cost effective method for producing coatings and spray formed components of $MoSi_2$ and $MoSi_2$-based composites. In this paper we will report on the use of plasma sprayed $MoSi_2$ as a potential coating over Al_2O_3 to replace platinum and the use of $MoSi_2$-Al_2O_3 spray formed composites to enhance the mechanical performance and damage tolerance of the protective sheath material.

3.0 Experimental

Atmospheric plasma spraying was used to produce $MoSi_2$ coatings on Al_2O_3 thermocouple sheaths and layered and graded thermocouple sheaths of $MoSi_2$ - Al_2O_3 composites. The plasma spray equipment used included a Praxair Surface Technologies SG100 plasma torch and two Model 1264 powder feed hoppers. The plasma torch was mounted on a Fanuc S10 6-axis robot. A LabView based computer control system was used to monitor and control the processing gases and the powder hopper-dispensing rate. Details on how the powder hoppers can be controlled to produce graded and layered microstructures are found in reference **[8]**. A closed end graphite tube (12.7mm OD x 9.5 mm ID) was used as a substrate for producing the $MoSi_2$-Al_2O_3 composite thermocouple sheaths. To determine the mechanical behavior of the graded $MoSi_2$-Al_2O_3 structures C-rings and four-point bend samples were machined from the material deposited on the graphite rods. C-ring samples were wire electro-discharge machined (EDM) out of the sprayed tube samples. The C-rings had an OD of 25.93mm, an ID of 12.8mm and a width of 10.76 mm. The critical $b/(r_o-r_i)$ ratio was 1.64, within the required range of 1 to 4. The C-ring samples were tested in diametrical compression using a hydraulic Instron test frame (Type 1331 with an 8500 Plus controller and a 10kN load cell), at a cross-head speed of 0.125 mm/min

(strain rate ~ 0.316 x 10^{-4} s^{-1}). Machine compliance was corrected using a standard Al_2O_3 sample of known stiffness. The C-ring samples were machined and tested in accordance with ASTM Standard C 1323-96. Four-point bend test samples 25mm long x 5mm wide x 2.5mm thick were also machined from plasma sprayed composites. The samples were (EDM) machined and surface ground (approximately .00254 mm per pass) using a 150 and 320 grit grinding wheel. Bend testing was performed in an Instron machine using a cross-head speed of 0.5 mm/min. The samples were tested in a hardened steel fixture which were supported on steel pins 19 mm apart. Loading was accomplished by two steel pins 9.5 mm apart. The four-point bend tests were carried out in accordance with ASTM standard C-1161/90. The maximum stress was calculated using the following equation:

$$\sigma_f = 3PL/4bd^2 \qquad (1)$$

where σ_f is the maximum stress in the sample, P is the maximum load at which the sample fractured, L is the support span length, b is the specimen width and d is the specimen thickness.

4.0 RESULTS

4.1 Layered Composites

Macrographs demonstrating the flexibility of using atmospheric plasma spraying to produce tubular layer composites of $MoSi_2$-Al_2O_3 are shown in **Figure 3**. The white phase is the Al_2O_3 and the dark phase is $MoSi_2$. Figure 3a, b and c show progressively thinner discrete layers of both $MoSi_2$ and Al_2O_3. The thickness of each layer is given in **Table 1**. Optimizing the microstructure of the composite layered structure will require a better understanding of the influence of the layer thickness and spacing of each phase. **Figure 4** shows the stress-strain behavior of $MoSi_2$-Al_2O_3 laminate composites tested at 1200 ^oC with varying volume fractions of each phase. Increasing the volume fraction of $MoSi_2$ will decrease the strength of the composite but will improve the fracture energy (area under the stress-strain curve) of the composite system. This improvement in fracture energy can be attributed to the brittle-to-ductile transformation that occurs in $MoSi_2$ at approximately 1000 ^oC **[9]**. For this composite system at temperatures above 1000 ^oC $MoSi_2$ acts like a ductile reinforcement for Al_2O_3 improving its damage tolerance at elevated temperatures. Investigations are currently being performed to understand the influence of the layer thickness on the mechanical and thermal properties of the composite and how this can effect the thermal shock behavior **[10].**

Crack mechanisms associated with a layered $MoSi_2$-Al_2O_3 composite are illustrated in **Figure 5a**. The advancement of a crack at elevated temperatures will depend on the layer thickness of the ductile $MoSi_2$ layer. Under an initial applied stress, cracks will be introduced stochastically in the Al_2O_3 layer. Crack advancement into the next brittle Al_2O_3 layer will occur at some critical applied stress intensity. Catastrophic crack advancement through the composite layers will be effected by the ability of the ductile $MoSi_2$ layers to provide bridging ligaments, crack deflection, and multiple cracking which can reduce the stress intensity at the tip of the advancing crack. The cracking behavior of a $MoSi_2$-Al_2O_3 composite after thermal shocking the composite from 900^oC to room temperature water is shown in **Figure 5b**. Multiple cracking occurred in the Al_2O_3 layers. The sample did not catastrophically fail after the thermal shock test.

4.2 Graded Composite

A cross-section of a continuously graded structure where pure Al_2O_3 was first deposited on a graphite mandrel followed by increasing amounts of $MoSi_2$ until pure $MoSi_2$ is deposited on the outside diameter of the spray deposited tube is shown in **Figure 6a**. A fracture surface of the continuously graded composite is shown in **Figure 6b**. When examining the fracture surface of a C-ring (which was sectioned from a spray formed tube) extensive microcracking and roughening was observed in the center portion of the C-ring. Load displacement curves for monolithic $MoSi_2$, Al_2O_3, a continuously graded $MoSi_2$-Al_2O_3 composite and a layer graded $MoSi_2$-Al_2O_3 composite showed that the monolithic material exhibited a low fracture energy ($MoSi_2$-496 J/m^2 and Al_2O_3 -285 J/m^2) compared to the continuously graded composite which exhibited the largest amount of fracture energy (955 J/m^2) versus the layered graded composite which had a fracture energy of 766 J/m^2, **Figure 7**.

4.3 $MoSi_2$ Coated Al_2O_3 Thermocouple Sheath

Results of plasma sprayed $MoSi_2$ coatings on Al_2O_3 thermocouple sheaths that were immersed in a molten alkali borosilicate glass at a temperature of 1550^{o}C is shown in **Figure 8**. Necking at the glass/air interface was observed in addition to pest oxidation that occurred in a region along the length of the $MoSi_2$ coated thermocouple sheath. Pest oxidation occurs in $MoSi_2$ at approximately 500 ^{o}C **[11]** when MoO_3 forms and causes the disintegration of $MoSi_2$. The pesting that occurs away from the molten glass does not effect the performance of the thermocouple sheath directly above and below the glass melt. The necking that occurred at the glass/air interface can be attributed to the loss of the protective SiO_2 layer on $MoSi_2$ and the high oxygen activity in this region **[3].** Methods to improve the performance of the glass/air interface are currently under investigation. The $MoSi_2$ coating above and below the glass line showed no indication of degradation from the molten glass. The protective nature of the SiO_2 layer above the glass melt and the Mo-rich coating below the glass melt enhanced the performance of the Al_2O_3 thermocouple sheath.

5.0 Conclusion

In this investigation we have demonstrated the use of conventional atmospheric plasma spraying for manufacturing layered and graded composites of $MoSi_2$-Al_2O_3. The mechanical performance of these composites was superior to that of the monolithic materials. This was verified through four-point bend, C-ring tests, and fracture characteristics. The protective nature of the plasma sprayed $MoSi_2$ due to the formation of SiO_2 and Mo-rich phases enhances the performance of the Al_2O_3 thermocouple sheath in molten borosilicate glass. Efforts to improve the corrosion rate at the glass/air interface are currently in progress.

6.0 Acknowledgements

This research has been supported by the U.S. Department of Energy, Office of Industrial Technologies, Advanced Industrial Materials Program, Glass Industry.

References

1. Report: Glass Technology Roadmap Workshop, Energetics Incorporated, April 24-25, 1997 pp. 21-29.

2. R.L. Anderson, Temperature: Its Measurements and Control in Science and Industry, American Institute of Physics, Ed. J.F. Schooley, Vol 5., (1982) 977-1007.

3. Y.S. Park, D.P. Butt, R. Castro, J. Petrovic, W. Johnson, *Mat. Sci. and Eng.,* A261, 278-283 (1999).

4. R. Tiwari, H. Herman, and S. Sampath, "Vacuum Plasma Spraying of $MoSi_2$ and its Composites," *Mat. Sci. Eng.,* A155 95-100 (1992).

5. A. Newman, S. Sampath, and H. Herman, "Processing and Properties of $MoSi_2$-SiC and $MoSi_2$-Al_2O_3," *Mat. Sci. Eng.,* A261 252-260 (1999).

6. H. Kung, R.G. Castro, A.H. Bartlett, and J.J. Petrovic, "The Structure of Plasma Sprayed $MoSi_2$-Al_2O_3 Microlaminate Tubes," *Scripts Metall. Et. Mater.*, 32 [2] 179-183 (1995).

7. R.G. Castro, J.R. Hellman, A.E. Segall, and D.L. Shellman, "Fabrication and Testing of Plasma-Sprayed Formed $MoSi_2$ and $MoSi_2$ Composite Tubes," *Mat. Res. Soc. Symp. Proc.*, 322 81-86 (1994).

8 M.I. Peters, R. U. Vaidya, R. G. Castro, J.J. Petrovic and K.J. Hollis, FUNCTIONALLY GRADED $MOSI_2$-AL_2O_3 TUBES FOR TEMPERATURE SENSOR APPLICATIONS"

9. K. Ito, K. Matsuda, Y. Shirai, H. Inui, and M. Yamagucji, "Brittle-Ductile Behavior of Single Crystals of $MoSi_2$," *Mat. Sci. Eng.,* **A261** 99-105 (1999).

10. Daniels Thesis

11. T.C. Chou and T.G. Nieh, "Pesting of the High-Temperature Intermetallic $MoSi_2$," *JOM* [12] 15-21 (1993).

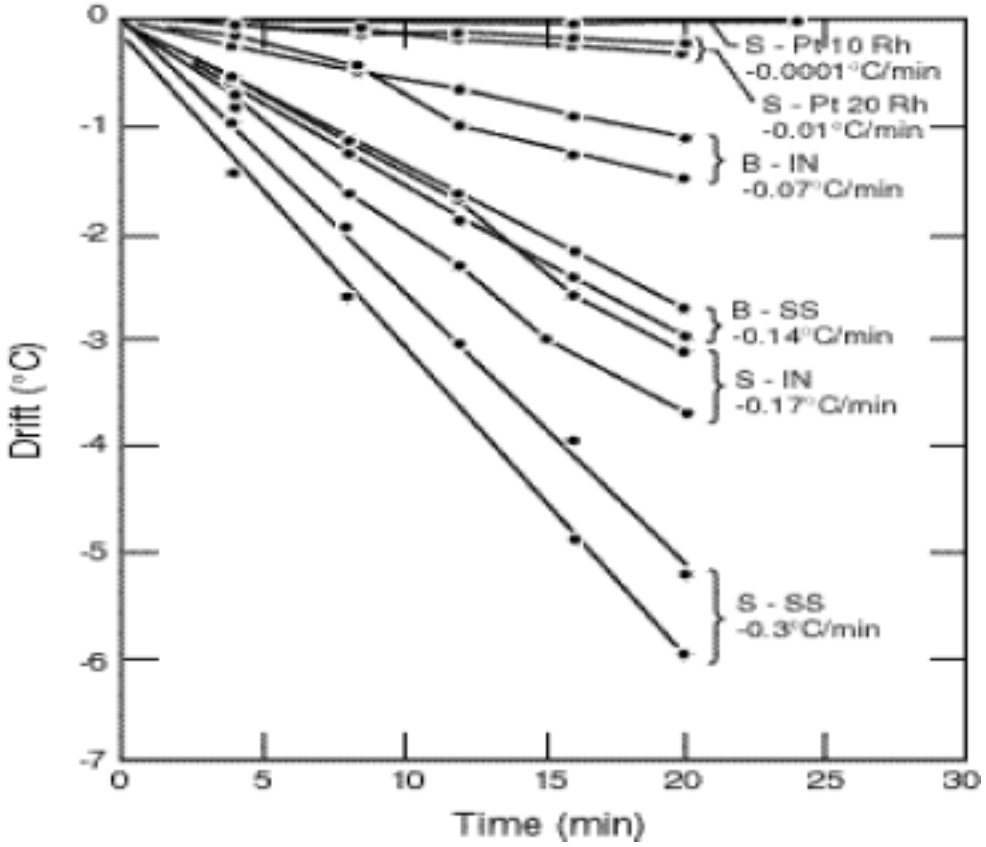

Figure 1. Drift in the indicated temperatures of small diameter, metal-sheathed noble-metal thermocouples measured at 1305 $_{o}$C over a period of 20 minutes. **[2]**

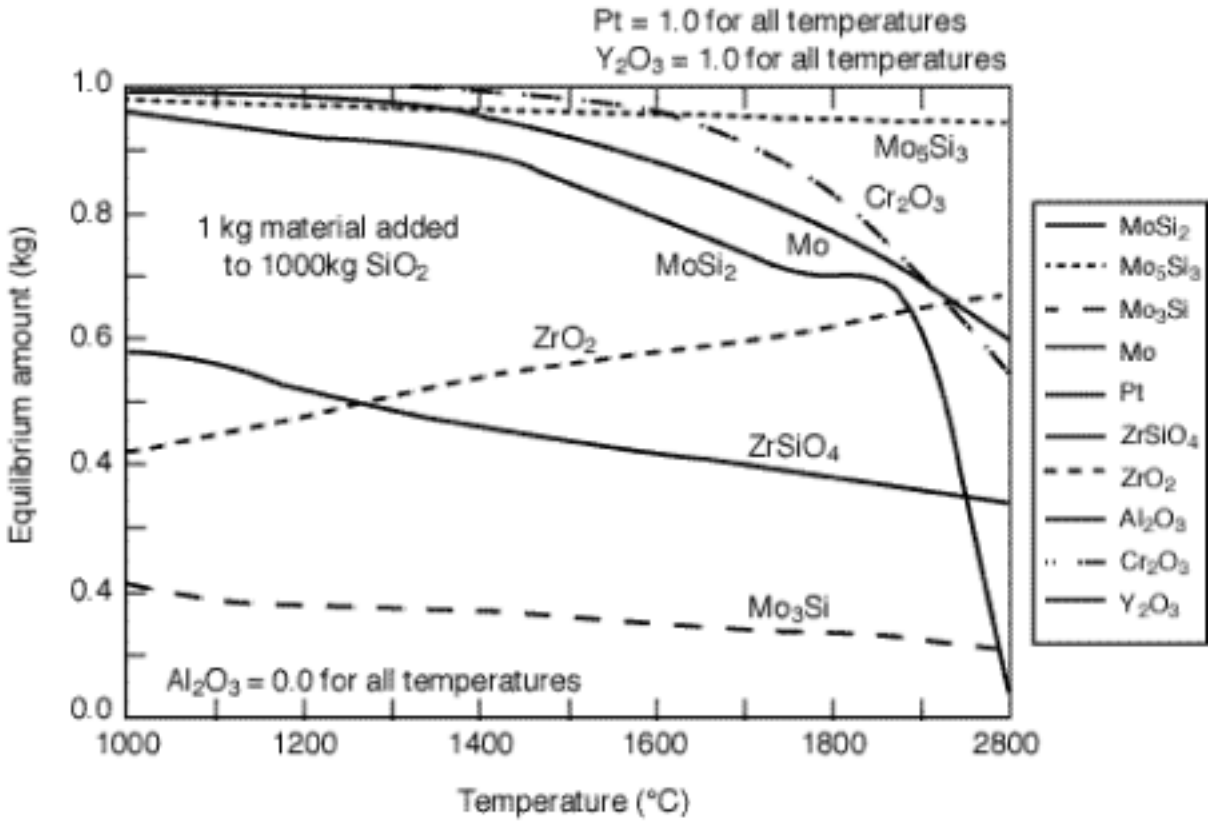

Figure 2. Equilibrium amounts of various materials in silica between 1000°C and 2800 °C.

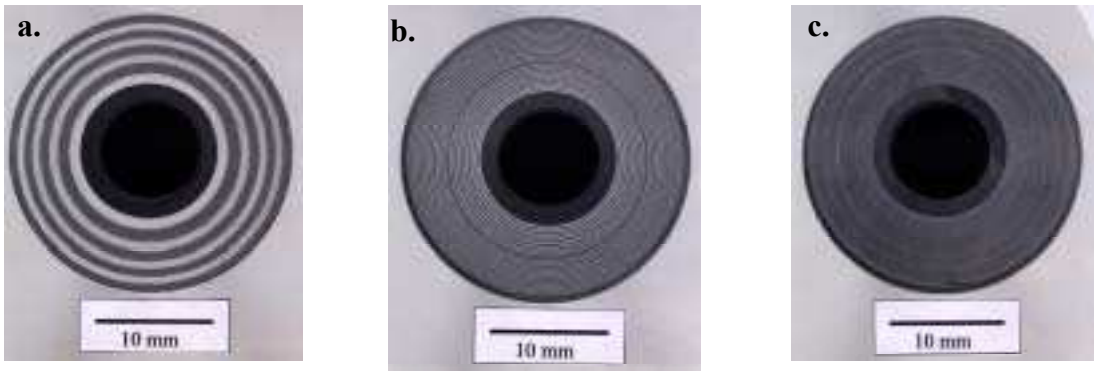

Figure 3. Macrographs of $MoSi_2$-Al_2O_3 layered composites.

Table 1.
Layer thickness for composite tube structures.

	$MoSi_2$ (μm)	**Al_2O_3** (μm)
Fig. 3a	49 ± 20	61 ± 20
Fig. 3b	226 ± 80	184 ± 50
Fig. 3c	670 ± 180	690 ± 100

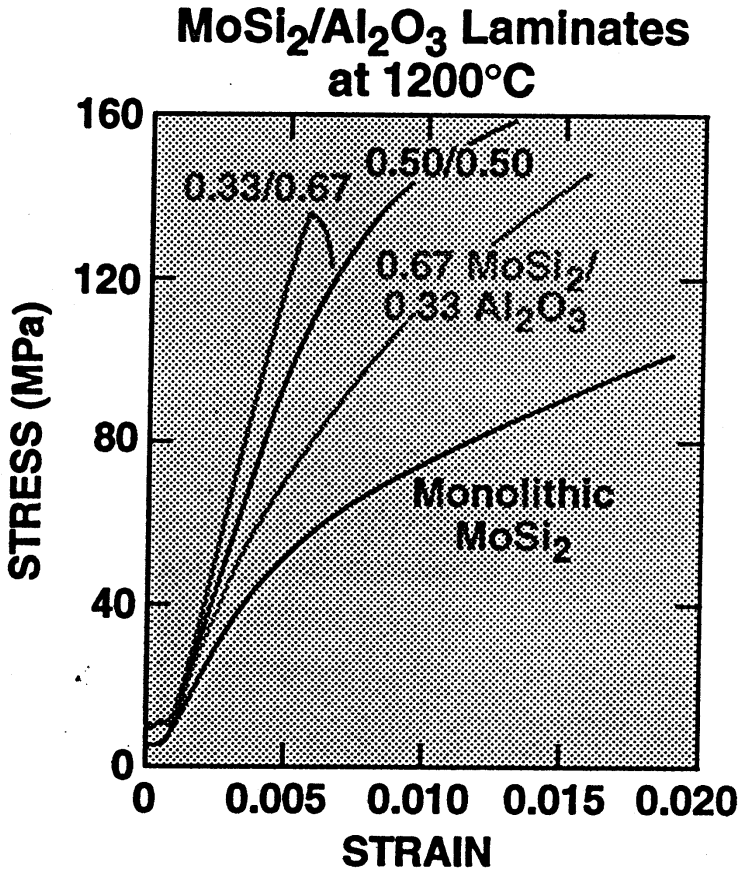

Figure 4. Stress-strain curve versus volume fraction of $MoSi_2$ and Al_2O_3.

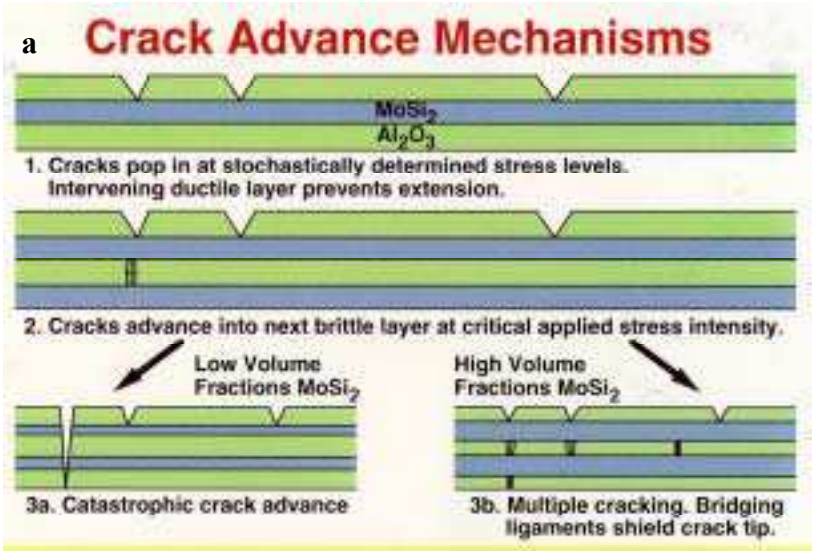

Figure 5. a) Crack advancing mechanisms for a $MoSi_2$-Al_2O_3 layered composite, b) multiple cracking in the Al_2O_3 layer after thermal shocking the sample from 900 ^oC.

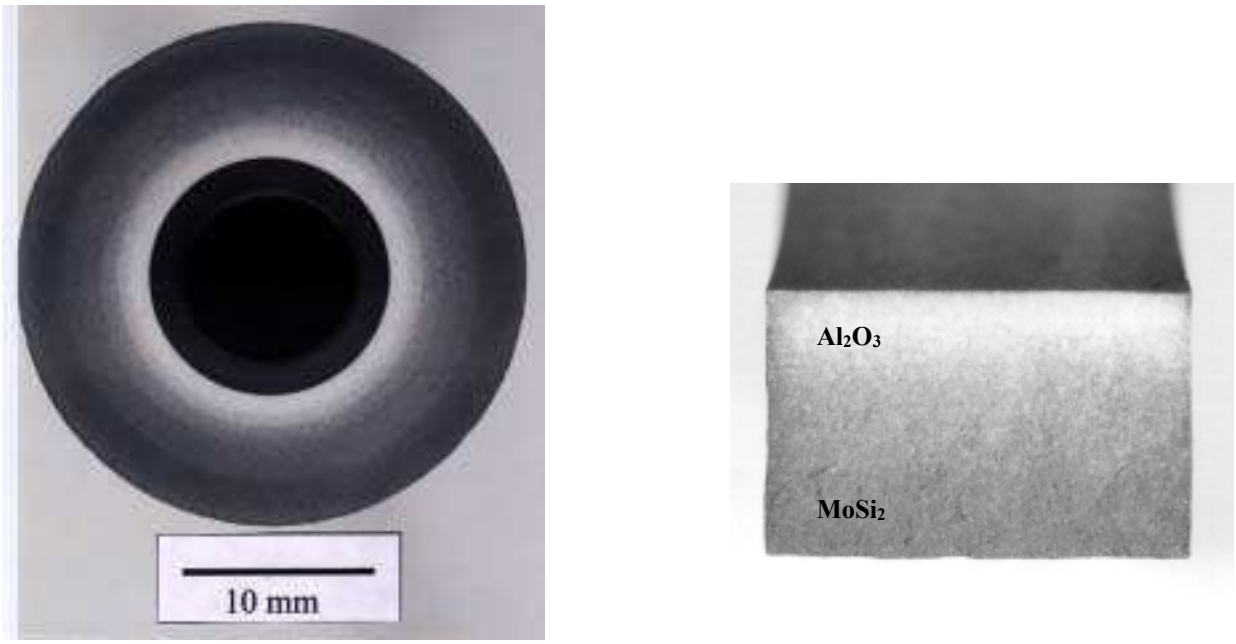

Figure 6. a) Cross-section of plasma sprayed $MoSi_2$-Al_2O_3 graded composite, b) fracture surface of a C-ring section.

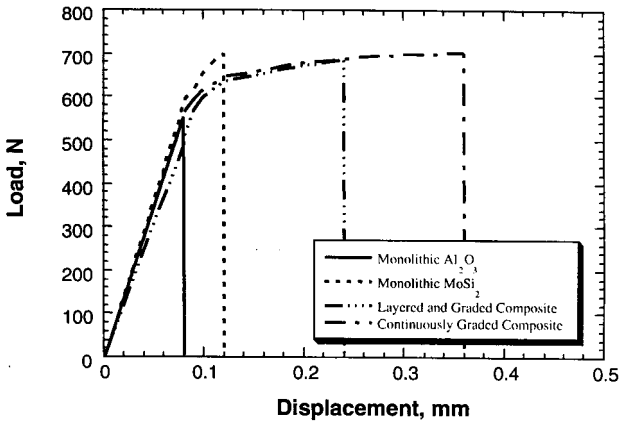

Figure 7. Work of fracture from load-displacement curves for monolithic $MoSi_2$, Al_2O_3, a continuously graded $MoSi_2$-Al_2O_3 composite and a layer graded $MoSi_2$-Al_2O_3 composite.

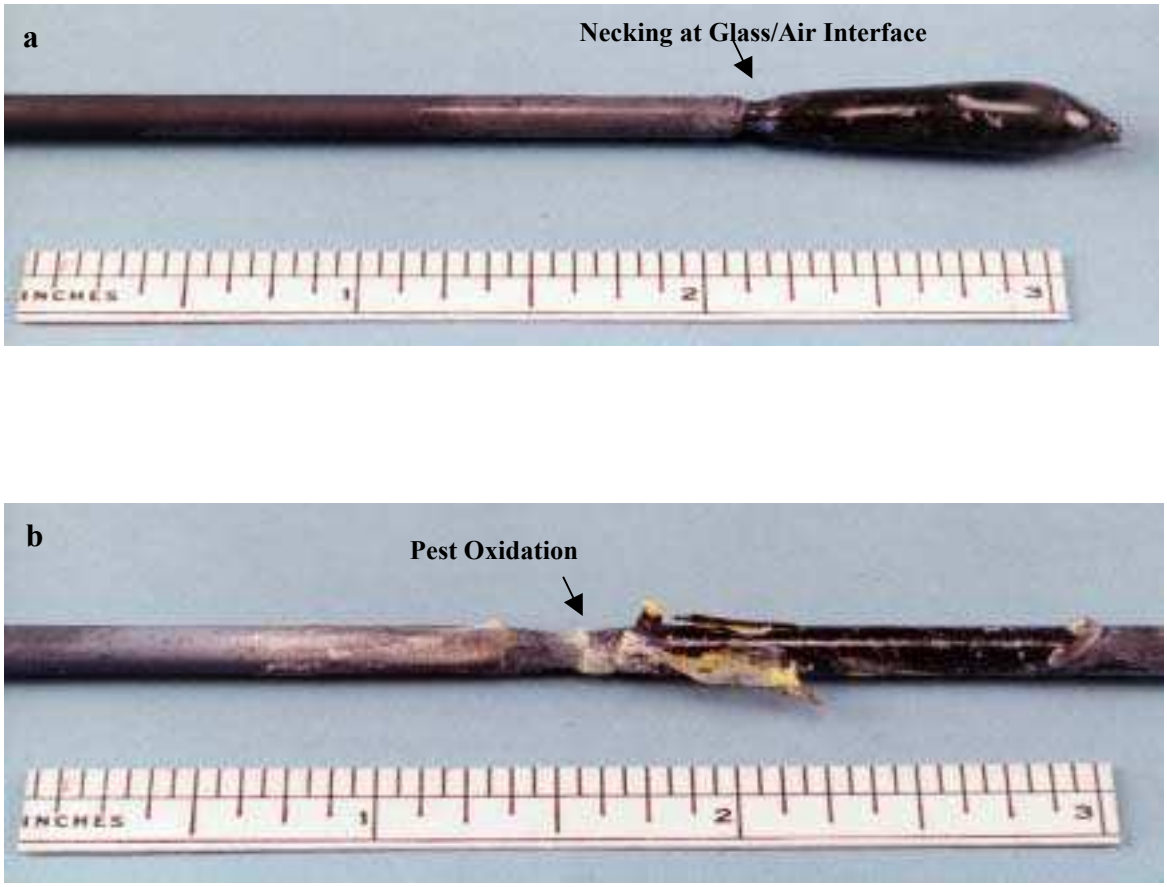

Figure 8. a) necking at the glass/air interface, b) pest oxidation that occurred in a region along the length of the $MoSi_2$ coated thermocouple sheath.